



Research paper

Analysis of traffic load effects in railway backfilled arch bridges

Tomasz Kamiński¹, Czesław Machelski²

Abstract: The problem of the arch barrel deformation in railway backfilled arch bridges caused by their typical service loads is analysed. The main attention is paid to vertical or radial displacements of characteristic points of the arch barrel. In the study results of deflection measurements carried out on single and multi-span backfilled arch bridges made of bricks or plain concrete during passages of various typical railway vehicles are used. On the basis of such results empirical influence functions of displacements are being created. In the next step, the results are utilised to estimate bending effects within the arch. The paper includes different procedures based on measurements of displacements in various points and directions. Using empirical influence functions arbitrary virtual load cases may be also considered. In this manner the proposed methodology shows a potential to be an effective tool of comprehensive calibration of numerical models of backfilled arch bridges on the basic of field tests carried out under any live loads.

Keywords: field testing, Finite Difference Method, Finite Element Method, influence lines, masonry arch bridge, numerical analysis

¹PhD., Eng., Wrocław University of Science and Technology, Faculty of Civil Engineering, Wyb. Wyspiańskiego 27, 50-370 Wrocław, Poland, e-mail: tomasz.kaminski@pwr.edu.pl, ORCID: 0000-0002-9023-3734

²Prof., DSc., PhD., Eng., Wrocław University of Science and Technology, Faculty of Civil Engineering, Wyb. Wyspiańskiego 27, 50-370 Wrocław, Poland, e-mail: czeslaw.machelski@pwr.edu.pl, ORCID: 0000-0002-1215-7908

1. Introduction

1.1. Fields load testing of backfilled arch bridges

Backfilled arch bridges (including both masonry and plain concrete ones) are complex structures characterised by many parameters having an important influence on their structural performance. Such an influence was studied in many field [1, 2] as well as full-scale laboratory [3–7] tests. These technical parameters cover both material properties of structural components (to be precisely defined in diverse laboratory tests) as well as their geometrical characteristics including those hidden by backfill and inaccessible for direct measurements. Therefore, in case of no technical data on a structure available, a precise determination of the structural features of backfilled arch bridges enabling their reasonable modelling and analysis is a difficult and time-consuming task.

There are many strategies developed and described in literature about how to establish such missing data through calibration of numerical models (defined by these sought parameters) on a basis of field testing results monitoring structure's response to different types of loads and actions. They include mainly a concentrated static loading located at different positions on a span or dynamic excitations developed by various sources. The former types of loads may be generated mainly by means of vehicles (preferably locomotives) [8] or (less commonly) by a heavy ballast put on a span [9]. In the latter group of loads impulse excited vibrations are generated by a mechanical device (exciter) [10], by walking [11] or jumping of a man [12], by passage of a vehicle over a bump (for road bridges) or in exceptional cases by hitting of a backhoe [13]. An additional large number of dynamic testing cases are based on ambient vibrations [11, 14, 15].

In most of these testing campaigns the main measured quantities are displacements and vibration accelerations recorded in the time domain. The collected data may be processed to get further information on structural behaviour providing a basis for a numerical model calibration. E.g. Pepi et al. [16] used Operational Modal Analysis (OMA) to get experimental modal characteristics (vibration modes and frequencies) of a masonry arch bridge from directly measured quantities and compared them to the corresponding values calculated by means of an FE model. Then, they carried out a manual tuning of the model to get the most representative values of parameters for modulus of elasticity and density of the main structural materials. This method was used also by Bayraktar et al. [11] but here the subject of the model calibration were just boundary conditions. The same approach as Pepi et al. was applied by Conde et al. [15] however the calibration process was partially defined as a nonlinear optimization problem and solved automatically. Also similarly did Costa et al. [14] but in this case the authors supported the calibration procedure with Genetic Algorithm (GA). Additionally, they considered three approaches related to different groups of the optimized material parameters and finally got very satisfactory results of the model tuning. Yazdani and Azimi [17] used a time-step dynamic analysis to compare precisely calculated bridge displacements in the time domain under railway traffic with the corresponding measured results and on this basis they adjusted material parameters of an FE model of a backfilled plain concrete arch bridge. Brencich and Sabia [13] through comparison of dynamic testing results with numerical analysis indicated a significant influence

of internal spandrel walls on the modal properties of a masonry arch bridge, in this way showing a method how to identify its unusual hidden geometry.

1.2. The proposed approach

The aforementioned techniques are very complex and time-consuming procedures, since the results of the measurements can be used as well in a more fundamental way. The approach proposed in this work to bridge performance monitoring is based on a study on deformations of the arch barrel under traffic actions considered as a quasi-static loads. In case of railway bridges, that kind of analysis can be especially effective taking into account symmetry and regularity of the traffic load scenarios. The concept is related to measurements of displacements on site and one of its main advantages is a possibility to carry out the tests during regular exploitation of bridges – without any disturbance to the traffic. Even if the displacement measurements are limited to a few points on a structure, the obtained results can provide comprehensive information on the structural response to many independent loading cases. Besides, simultaneous recording of displacements in a few points may additionally provide more complete information on the internal effects within the structure. Thus, such kind of tests may be an efficient tool of a backfilled bridge model calibration verifying it in a global way.

The proposed analysis is presented in a few case studies of railway arch bridges with different numbers of spans. Effects of various railway vehicle types crossing them at different speeds are controlled and registered what provides more comprehensively verifying data used in further calibration process. The presented testing campaigns are carried out for passages of vehicles at generally low velocities, therefore the dynamic effects are small and the loads may be treated as quasi-static. Generally, in case of backfilled arch bridges with large mass and damping ratio [18] and especially those with very low or no piers the dynamic influences on their load carrying capacity are relatively limited [19].

The displacements are measured at intrados of the arch barrels. Displacements and strains at the supports' basis level for such massive structures is assumed to be negligible. The measurements are carried out mainly by means of LVDT gauges installed on steel tripods located under the bridge and additionally verified by means of laser vibrometer and microradar equipment. Selected details of the sensors' arrangement are shown in Fig. 1.



Fig. 1. Details of the sensors' arrangement: a) an LVDT gauge, b) tripods, c) combined systems

On this basis, influence lines of these displacements are being created. From the variation of the curvature of the arch one can get bending moments. In the analysis the elastic response of the structures is assumed since the range of stress variation coming from the considered traffic loads is relatively low and no cracking, material yielding nor any symptoms of nonlinear behaviour occurs.

The bridges considered in this work are shown in Fig. 2. They belong to two groups: "A" – single-span and "B" – multi-span structures. The basic geometrical parameters related to the arch barrel intrados are presented in Table 1. Namely, they are: R – radius of the arch, L_0 – clear span, H – rise of the arch at the crown, B – width of the arch barrel h – depth of the arch barrel. Bridges in Milicz and Oleśnica are fully made of bricks. The bridge in Świdnica has a brickwork arch barrel but its spandrel walls and arch faces are made of stone. The estacade in Strzegom is a plain concrete one. The technical condition of the structures is rated as good – no significant damage is observed.

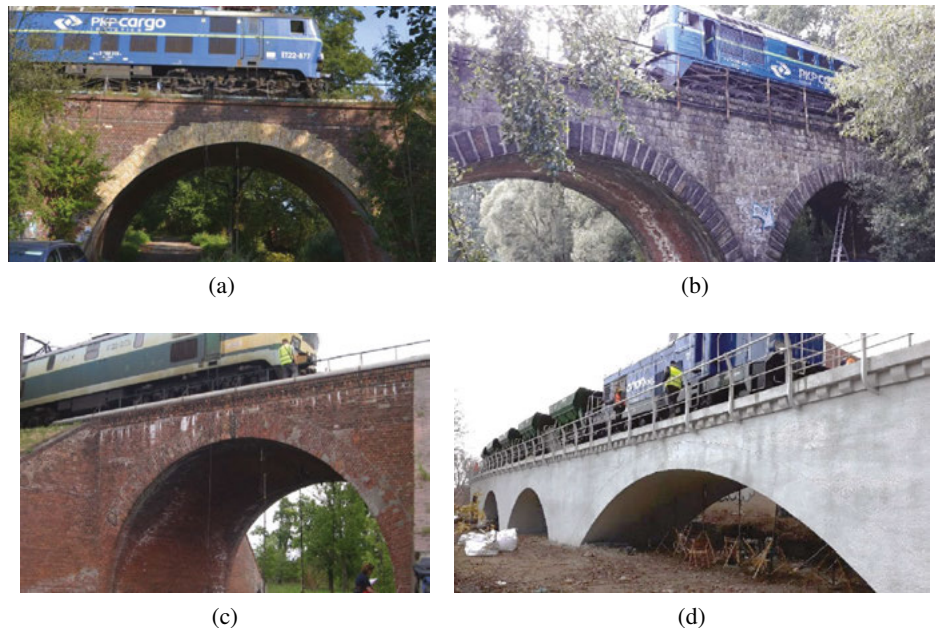


Fig. 2. The analysed backfilled arch bridges in: a) Milicz, b) Oleśnica, c) Świdnica, d) Strzegom

Table 1. Geometrical parameters of the analysed bridges

Type	No. of spans	Name	R [m]	L_0 [m]	H [m]	B [m]	h [m]
A	one-span	Milicz	6.00	12.00	6.00	8.55	0.80
		Oleśnica	4.97	9.94	4.97	8.55	0.78
B	two-span	Świdnica	5.438	10.00	3.30	4.82	0.75
	multi-span	Strzegom	13.385	16.64	2.887	4.08	0.71

2. Deflection of the arch crown caused by crossing of railway vehicles

The analysed bridges of the type “A” were built on the same railway line in 1875 (Fig. 2a, 2b). They belong to the same geometric group of semi-circular arches. In these objects the analysis is focused on the arch crown deflection at three points distributed across the bridge width. By means of such measurements the contribution of the entire width of the arch in transferring the railway load may be evaluated.

Fig. 3a presents an example of measuring the deflection at the mid-span of the arch averaged from such three points during the passage of a train, i.e. a locomotive with wagons. The diagram shows the effect of ET22 locomotive load in the form of two extreme values of displacement resulting from the action of the bogies of the vehicle – each composed of three axles. The space between the extreme values is the result correspond to the distance between the bogies in the locomotive. Also in the case of wagons, the influence of individual axles, e.g. in double axle systems, is not visible. However, the spacing of the bogies of a given wagon is clearly identifiable, while the spacing between bogies in subsequent wagons is slightly visible in the diagram. At the same axle loads, the second extreme may be greater, as in Fig. 3a, as the result of the influence of forces coming from the wagon attached directly to the locomotive. In the example, the wagons are empty. Similar types of diagrams for such measurement results are found by other authors [20, 21].

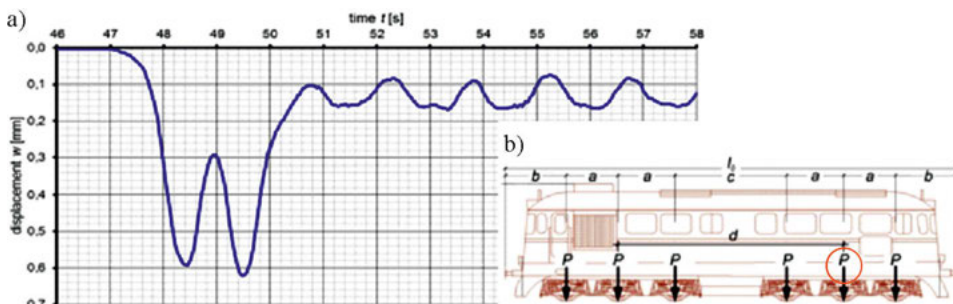


Fig. 3. a) Changes in the deflection of the arch during a train passage in Milicz, b) geometrical parameters in the considered locomotives (reference axle indicated)

The graph presented in Fig. 3a is a function of the arch crown deflection in the time domain, $w(t)$. Important for static analysis is the conversion of this function into a form tracking the position of the load x . For this purpose, the function $w(t)$ is transformed into $w(x)$. In the paper, x is the distance between the middle force of the front locomotive bogie (indicated in Fig. 3b) and the crown section. Thus, $x = 0$ is taken for the first extreme value $w(t)$ and on this basis the value t_o is chosen. Assuming that the distances between the bogie axles d are consistent with the formation of extreme deflection values, the travel speed v can be determined. The basic technical parameters of all the locomotives considered in the study are given in Table 2.

Table 2. Technical parameters of the considered locomotives

Locomotive type	P [kN]	a [m]	c [m]	b [m]	d [m]	l_0
ET22	200	1.75	6.80	2.72	10.30	19.24
ST44	196.2	2.10	4.40	2.375	8.60	17.55
Dragon	202.2	1.95	6.60	2.965	10.50	20.33

When the travel speed v is stable, the transformation of the function $w(t)$ into the location domain x is carried out according to the Eq. (2.1):

$$(2.1) \quad w(x) = V \cdot w(t - t_0)$$

The diagrams $w(x)$ for bridges in Milicz and Oleśnica are shown in Fig. 4 and Fig. 5, correspondingly.

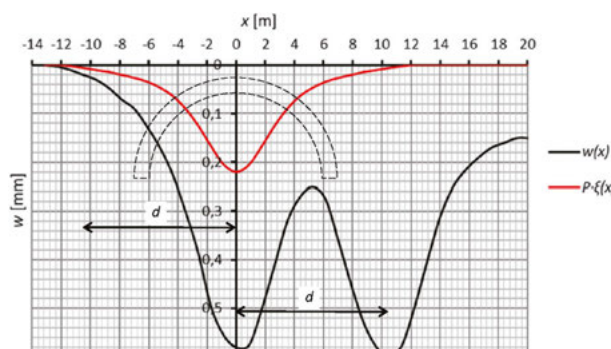


Fig. 4. The measured deflection variation $w(x)$ from the passage of ET22 locomotive and the influence function $\xi(x)$ (presented rescaled by force P) for the bridge in Milicz

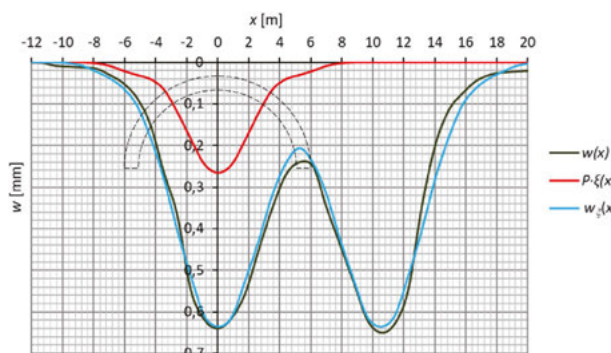


Fig. 5. Directly measured $w(x)$ deflection variation from the passage of ET22 locomotive and calculated $w_\xi(x)$ from the influence function $\xi(x)$ (presented rescaled by force P) for the bridge in Oleśnica

In the presented testing campaigns, the travel speeds of the locomotives (trains) were between 10 and 19 m/s. Due to low values of the dynamic amplification factor in these bridge structures, such passages can be considered quasi-static. However, for higher dynamic amplification the measured results may be simply filtered to extract the static component of displacements.

3. Influence line of displacement

The diagrams $w(x)$ can be further used to create empirical influence functions of the arch crown deflection $\xi(x)$. For this purpose constant axle load values P given in Table 2 for each case are assumed. Accordingly, a general relationship between the arch crown deflections $w(x)$ and ordinates $\xi(x)$ of the influence function corresponding to the location of the successive locomotive axles defines Eq. (3.1):

$$(3.1) \quad w(x) = P \sum_{i=1}^n \xi(x + x_i)$$

where: x – location of the locomotive reference axle against the arch mid-span section, x_i – location of the consecutive locomotive axle i against the reference axle, n – the number of the locomotive axles.

To find the values of the influence function $\xi(x)$ a progressive calculation procedure is applied starting from the point $x = x_0$, for which the whole measured deflection is equal to $w(x_0)$ while for all the previous points laying at least in distance a from x_0 it is equal to $w(x_0 - a) = 0$. Thus, at the beginning of the analysis the initial position of the first axle load is considered as follows:

$$(3.2) \quad w(x_o) = P \cdot \xi(x_0 + a)$$

From Eq. (3.2) the function value $\xi(x_0 + a)$ can be calculated taking into account $\xi(x_0) = 0$. The second function ordinate is calculated for a point in distance a from the previous one, according to Eq. (3.3):

$$(3.3) \quad w(x_o + a) = P [\xi(x_o + a) + \xi(x_o + 2a)]$$

Further procedure carried out with subsequent positions of the locomotive allows to find the next ordinates of the influence function $\xi(x)$.

Fig. 4 and Fig. 5 present also the shape of the deflection influence functions $\xi(x)$ calculated according to the described procedure for the bridges in Milicz and Oleśnica, correspondingly. However, in the second case the diagram is obtained on the basis of ET22 locomotive crossing the bridge without wagons. For the compatibility of the units with the diagrams $w(x)$ the ordinates ξ are multiplied by axle load P treated here as a constant factor. In case of a single locomotive crossing a bridge the confirmation of the influence function $\xi(x)$ correctness should be the agreement between diagram $w_\xi(x)$ developed backward

from $\xi(x)$ with the diagram of the directly measured deflections $w(x)$ – as it is presented also in Fig. 5 – according to the Eq. (3.4):

$$(3.4) \quad w(x) \cong w_\xi(x) = P \sum_{i=1}^n \xi(x + x_i)$$

The results obtained in both cases are very similar. A characteristic feature of these “A” type structures is the fully positive deflection line, as in Fig. 2a, and resulting from it the similar shape of the deflection influence lines. In case of “B” type bridges, this characteristics is different.

4. Case study of a twin-span masonry arch bridge

The bridge in Świdnica was built in 1897 with twin brickwork arches of a segmental shape. In this bridge an important role play massive stonework spandrel walls (Fig. 2c). They constitute a very stiff load-bearing structure undergoing lower displacements than bridges described above. Fig. 6a shows the deflection functions of three points from the circumferential line of the arch intrados obtain during field measurement. Point K relates to the crown, while points A and B are distant from the crown by $L_0/4 = 2.5$ m. From the comparison of the deflection diagrams given in both Fig. 4 and Fig. 5 with Fig. 6, a difference is visible in the form of the negative deflection branch on the side of the adjacent span. For this reason, the bridge is classified as group “B” because in the case of structures of the type “A” these lines are fully positive. Therefore, in multi-span systems a different graph should be expected than in the case of structures in the form of a single arch.

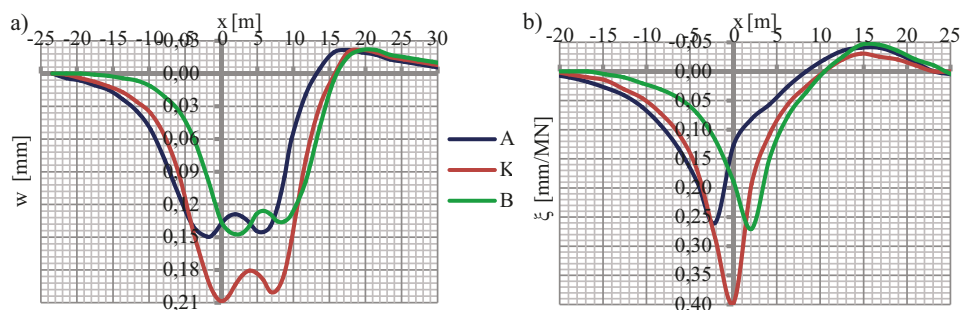


Fig. 6. Results from Świdnica: a) deflection variation $w(x)$ under ST44 loco, b) influence lines of deflection

Based on the geometry of the used ST44 locomotive (given in Table 2) and the deflection diagrams $w(x)$, the influence lines of deflection $\xi(x)$ presented in Fig. 6b are created. The procedure given in Section 3 is used for this purpose. In the case of the bridge in Świdnica, diagrams are also created for intermediate points marked as A and B. From the comparison of the graphs in Fig. 5 and 6, the effect of the adjacent span is very clear, both in the

graphs $w(x)$ as well as on the influence lines of deflection $\xi(x)$. On this basis, the analysed structures are classified as two different types.

5. Estimation of bending effects in masonry arches

When measuring displacements at several points located along the circumferential line of the arch intrados, it is possible to estimate the change in the radius of curvature [24]. For this purpose, the *Finite Difference Method FDM* [25] and displacements with radial direction (consistent with the radius of curvature R) are used as in Fig. 7.

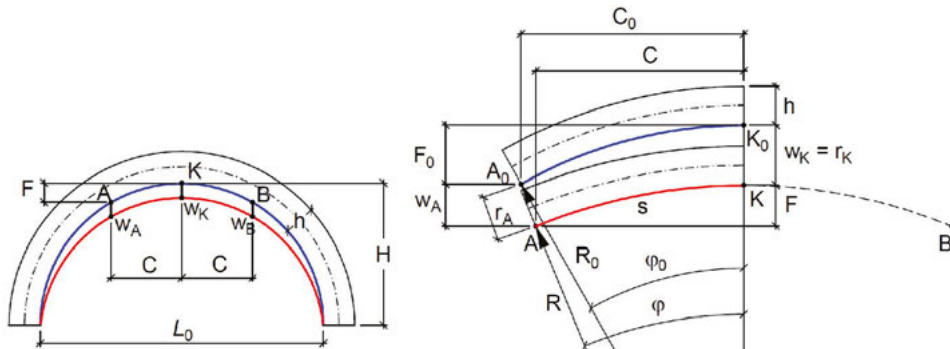


Fig. 7. Diagram of deformation of the arch segment at crown

Thus, for the central point K , the following relationship (Eq. (5.1)) is obtained:

$$(5.1) \quad \kappa = \frac{1}{s^2} \left\{ r_A - \left[2 - \left(\frac{s}{R} \right)^2 \right] r_K + r_B \right\}$$

where: s – the arc length from each measurement point A and B in relation to K .

Fig. 7 shows the direct measurement results in the form of the vertical displacements of the arch barrel w_A , w_K and w_B . In the sketch, a deformation diagram of an arch separated section with the displacements in the radial direction r_A and r_K occurring in the Eq. (5.1) are given also. Dimensions with the index '0' refer to the situation before deformation of the arch caused by loading. Since the measurements of displacements are carried out in the test for the vertical components only, the transformation of displacements from vertical (w) to radial (r) form is used for intermediate points A and B with the use of the Eq. (5.2) illustrated in Fig. 7:

$$(5.2) \quad r_A = \frac{R}{R - F} w_A$$

Dimensions of the arch segment F and C from Fig. 7 are geometrically related to the radius R :

$$(5.3) \quad R = \frac{F^2 + C^2}{2F}$$

For the analysed structure in Świdnica the geometrical parameters are as follows: $C = L_0/4 = 2.5$ m and $F = 0.609$ m (calculated from Eq. (5.3)). The arc length s given in Eq. (5.1) is:

$$(5.4) \quad s = R \cdot \varphi = 2R \cdot \arctan \left(\frac{F}{C} \right)$$

where the angle φ is defined in a radial form. Thus, the length of the arc between points A and K or K and B is $s = 2.597$ m. In Eq. (5.1) it is assumed that the deformation of the arch barrel is very limited and does not cause significant changes in geometry [22] therefore, the relationship $\varphi \approx \varphi_0$ is valid as well as the radius of the arch is treated as constant, so $R \approx R_0$.

After introducing the measurement results, i.e. vertical displacements of points A , K and B , a change in curvature in the crown section is obtained, as in the Eq. (5.5):

$$(5.5) \quad \kappa = \frac{R}{(R - F)s^2} \left\{ (w_A + w_B) - \frac{R - F}{R} \left[2 - \left(\frac{s}{R} \right)^2 \right] w_K \right\}$$

Then, it may be used to calculate the moment value taking into account the flexural stiffness of the arch as follows:

$$(5.6) \quad M(x) = EI \cdot \kappa(x)$$

Fig. 8 shows a diagram of the bending moment $M(x)$ in the crown section of the arch obtained from the passage of ST44 locomotive over the bridge in Świdnica for stiffness $EI = 254$ MNm² (assuming a typical value of the brickwork masonry modulus of elasticity). For the calculations the deflections at the intermediate points A , K and B presented in Fig. 6a were used. In turn, the diagrams of the influence line of deflection $\xi(x)$ for points A , K and B can be used to create influence lines of bending moment $\mu(x)$. According to the Eq. (5.5), if the deflections w_i are substituted for the ordinates of influence line of deflection ξ_i , one can obtain the Eq. (5.7):

$$(5.7) \quad \mu = \frac{R \cdot EI}{(R - F)s^2} \left\{ \xi_A + \xi_B - \frac{R - F}{R} \left[2 - \left(\frac{s}{R} \right)^2 \right] \xi_K \right\}$$

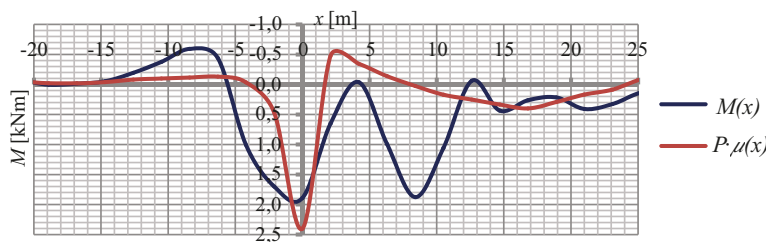


Fig. 8. Variation of the bending moment $M(x)$ during passage of a locomotive and the influence line $P \cdot \mu(x)$

Such an influence line of bending moment is also shown in Fig. 8 in a form $P \cdot \mu(x)$ (where the factor P is a single axle load of the locomotive) providing the same scale and units as the $M(x)$ diagram. In the graph the influence lines of deflection at points A , K and B (as in Fig. 6b) are used. Thus, all the presented functions are obtained on the basis of the deflections generated during the passage of the locomotive as in Fig. 6a. The advantage of the proposed approach is to obtain bending moments in the crown on the basis of measuring the displacement only in three points.

6. Case study of a multi-span concrete arch bridge

The analysed railway estacade in Strzegom is an example of a multi-span plain concrete arch. The geometrical parameters of the structure are summarized in Table 1. As before, the methodology of examining the bridge response assumed continuous measurement of displacements, but this time in the radial direction, hence the $r(t)$ functions is introduced. Measurement points are placed at regular horizontal intervals every $C = L_0/8$ along the circumferential line, as shown in Fig. 9. For this reason, the arc lengths between the measurement points marked as s_{ij} are variable. Table 3 presents the geometrical characteristics (described also in Fig. 9) for the location of the measurement points 0–2 in relation to the crown section $K = 3$. F_j can be found on the basis of defined R and C_j values using Eq. (5.3), while s_{ij} is calculated as the difference of S_j and S_i which are determined by Eq. (5.4). For the remaining point (with $j > 3$) a symmetry against the given ones can be noticed.

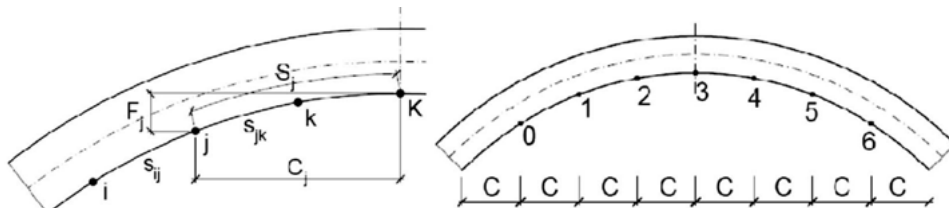


Fig. 9. Geometrical characteristics of measurement points for the bridge in Strzegom

Table 3. Geometrical characteristics for the location of measurement points of the bridge in Strzegom

Point j	C_j [m]	F_j [m]	S_j [m]	s_{ij} [m]	α [-]
0	6.24	1.5435	6.4917	2.2614	–
1	4.16	0.6629	4.2303		
2	2.08	0.1626	2.0881	2.0881	1.0259
3	0	0	0		

The different lengths of the arcs along the circumferential line are taken into account by the parameter α . For j -th point the value of $\alpha = s_{ij}/s_{jk}$ which is the ratio of the arcs length between points $i - j$ and $j - k$ (see Fig. 9). Thus, Eq. (5.1) is transformed to the Eq. (6.1):

$$(6.1) \quad \kappa_j = \frac{2}{\alpha(1+\alpha)s^2} \left\{ \alpha \cdot r_i - \left[(1+\alpha) - \alpha \left(\frac{s}{R} \right)^2 \right] r_j + r_k \right\}$$

Using Eq. (5.6) and (6.1) the bending moments can be calculated. Fig. 10 shows the diagrams of displacement measured in points 0–5 (point 6 showed erroneous results). The load in these tests is a rail excavator weighing 20 tons. The weight of the excavator is distributed between its axles in an unknown proportion. In this case, $x = 0$ is assumed for the maximum value of r_3 in the crown section. Based on the travel speed $v = 9.24$ m/s, the $r(t)$ graphs are transformed into $r(x)$ functions. Based on the displacements in the radial direction, the variation of bending moments $M(x)$ for points 1–4 is calculated and presented in Fig. 11, assuming $EI = 6045$ MNm 2 . The figure shows extreme values of the bending moments in similar positions as in case of displacements of the corresponding points. These charts are complemented by diagrams of bending moment distribution $M(s)$ along the circumferential line of the arch triggered by vehicle located in discrete position at x equal from -3.6 m up to 3.6 m every 0.8 m – see Fig. 12. The position of the load x [m] given in the legend of the figure, is counting from the crown section. The analysis area

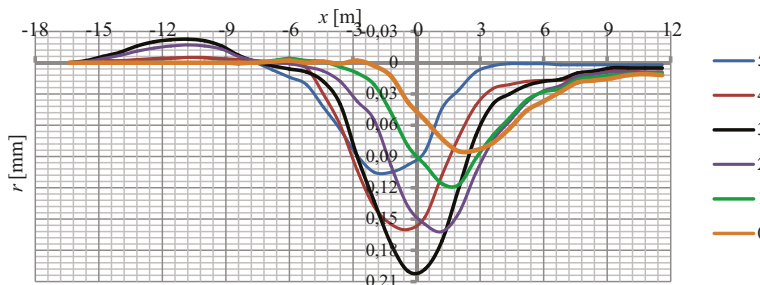


Fig. 10. Plots of radial displacements of measurement points for the bridge in Strzegom

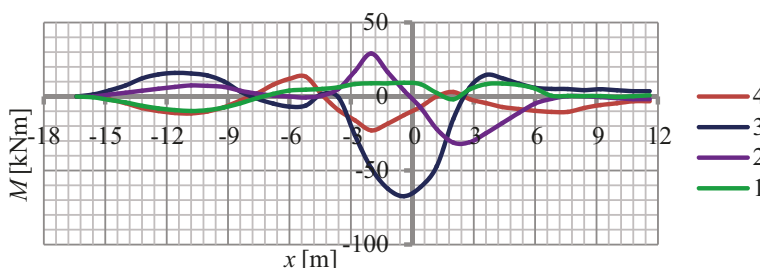


Fig. 11. Variation of bending moments $M(x)$ in selected points 1–4 as a function of the load position

concerns the side of the arch from where the vehicle is approaching the bridge ($x < 0$) as well as the other side of the arch ($x > 0$). Observing the shape of the $M(s)$ distribution the loading vehicle position may be estimated.

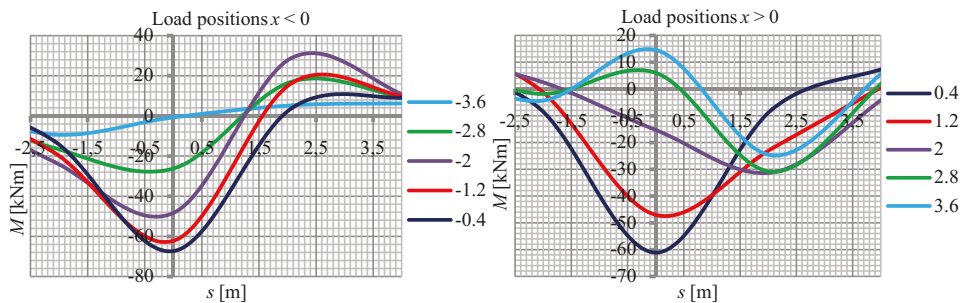


Fig. 12. Bending moment distributions $M(s)$ in the area of the arch crown section for the analysed discrete positions of the vehicle

7. Numerical modelling of masonry bridges

The previously presented examples of processing the measured displacements into influence lines and bending moments can be the basis for the calibration of parameters of the numerical model of a structure. In the study, the testing results for the bridges in Milicz and Oleśnica are used to demonstrate such a procedure. In this case, it is useful to consider the testing methodology based on a vehicle passage, which gives the possibility of obtaining many results at various characteristic load positions. It is particularly advantageous to represent the measurement results in the form of an influence line, which then allows comparison of various solutions e.g. when using a single concentrated force or any other arbitrary load scenario.

Two-dimensional FEM models are used in the analysis of both considered bridges, each of which represents the effective width of the structure corresponding to a single track. They are composed of a masonry arch barrel, masonry backing, soil backfill and pavement layer (see Fig. 13). The range of each model covers an area of the soil approximately 20 m from the arch on both sides to accommodate the most distant locations of the moving loads. The boundary condition at the bottom edge of the model limit all displacements while at

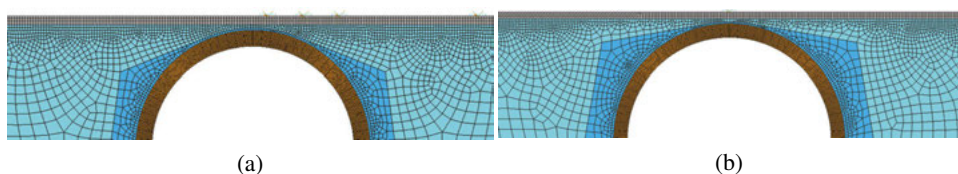


Fig. 13. FE models of the analysed bridges: a) in Oleśnica and b) in Milicz

the sides of it the horizontal ones only are blocked. The model is composed of 4-node plane strain solid finite elements with linear shape functions.

The masonry arch barrel is modelled with application of so-called mezomodelling technique [26] related to direct representation of selected radial masonry joints of the arch and using average (homogenized) masonry properties to the remaining segments separated by the joints. The homogenization process combining average strains and average stresses is applied in consecutive steps along 2 orthogonal axes of a representative volume element (RVE) of masonry according to [27]. The material of the masonry joints is defined by the *Concrete Damaged Plasticity* model available in the applied *ABAQUS* software with significantly limited (down to 0.05 MPa) tensile strength. The backfill material is simulated using the Drucker-Prager model (considering friction and dilatancy angles as well as cohesion). The properties of the materials are initially determined by means of field and laboratory testing and then adjusted on the way of numerical calibration based on the presented loading test results. Since the numerical model detailed description is not the essential subject of this study farther details on it can be found in [8]. The live load represents action of the locomotive axles – each of them is applied to the top of the pavement layer as a uniformly distributed pressure.

The carried out analysis concentrates on the tracking of the deflection of the arch barrel. Various loading scenarios are considered including: action of a single axle located every 1 m along the whole pavement of the model – to create a model-based influence line of deflection as well as the action of particular locomotives at the positions corresponding to those recorded during the measurements.

Two essential types of the analysis results are compared with the corresponding measured values:

- the influence lines of deflection in the arch midspan (presented in Fig. 14 for the bridge in Milicz in a factored form $P \cdot \xi(x)$) – created on the basis of individual analyses for various position of a single axle load $P = 250$ kN,
- deformation of the whole arch (presented in Fig. 15 for bridges in Oleśnica and Milicz) – triggered by the selected positions of the locomotives ET22 and Dragon, respectively.

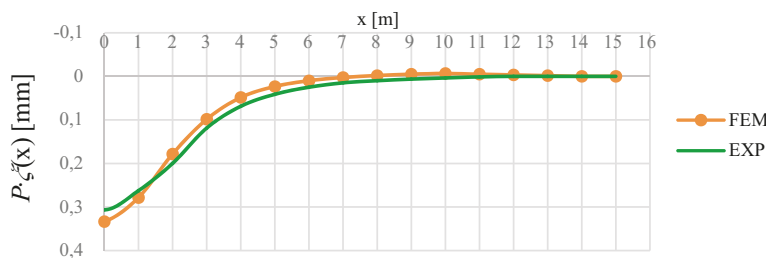


Fig. 14. Comparison of the factored influence lines $P \cdot \xi(x)$ for bridge in Milicz (loaded with the axle load $P = 250$ kN) obtained experimentally and from FEM analysis

In case of the calculated overall deformation of the arch barrel itself (presented in Fig. 15 along with the deformation of the surrounding backfill) its agreement with the

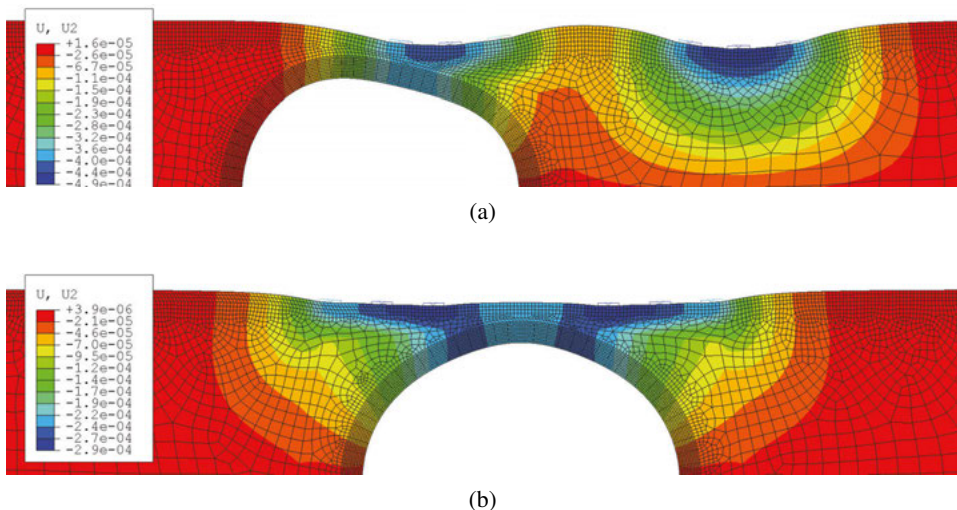


Fig. 15. Deformation calculated by means of FE models. a) for the bridge in Oleśnica under ET22 locomotive. b) for the bridge in Milicz under symmetric position of a DRAGON locomotive

measurement results possible to be reached on the way of the model calibration exceeded 95% on average, considering different vehicles and their positions.

8. Summary

The article presents selected case studies of loads effects generated by railway vehicles travelling across backfilled arch bridges. For a broader discussion of the spectrum of load effects, a slightly different methodology of measuring and processing of their results are presented in each analysed case. The possibility of estimating the effects of the arch bending on the basis of displacements is also indicated. The presented procedure of testing and analysis of arch bridge deflections under live loads may be an effective method of a comprehensive calibration of bridge numerical models including verification of the assumed material properties, invisible geometry or in case of a 2D model its effective width. The opportunity to get sufficient results from measurements carried out during regular exploitation of a bridge without any disturbance to the traffic is very attractive and in many situation makes the testing possible at all. The proposed approach is especially useful in analysis of railway bridges undergoing very regular and easily characterized loading schemes, like those represented by locomotives. However it can be also used in analysis of road bridges. The procedure can be based as well on other mechanical effects (including both vertical and horizontal displacements or strains) in any point of a structure.

References

- [1] T.E. Boothby, V.A. Dalal, "Service load response of masonry arch bridges", *Journal of Structural Engineering*, 1998, vol. 124, no. 1, pp. 17–23, DOI: [10.1061/\(ASCE\)0733-9445\(1998\)124:1\(17\)](https://doi.org/10.1061/(ASCE)0733-9445(1998)124:1(17)).
- [2] J. Page, *Masonry arch bridges*. London, UK: HMSO, 1993.
- [3] C.A. Fairfield, D. Ponniah, "Model tests to determine the effect of fill on buried arches", *Proceedings of the Institution of Civil Engineers: Structures and Buildings*, 1994, vol. 104, pp. 471–482, DOI: [10.1680/istbu.1994.27205](https://doi.org/10.1680/istbu.1994.27205).
- [4] T.G. Hughes, M.C.R. Davies, P.R. Taunton, "The influence of soil and masonry type on the strength of masonry arch bridges", in *Proceedings of the 2nd International Arch Bridge Conference – Arch Bridges: History, analysis, assessment, maintenance and repair*, 1998, pp. 321–330, DOI: [10.1201/9781003078494-46](https://doi.org/10.1201/9781003078494-46).
- [5] P. Krajewski, Z. Janowski, "The influence of backfill type on the behaviour of barrel vault", *Technical Transactions*, 2011, vol. 19, pp. 187–204. [Online]. Available: <http://repozytorium.biblos.pk.edu.pl/resources/35434>. [Accessed: 10. Nov. 2021].
- [6] M. Gilbert, F.W. Smith, J. Wang, P.A. Callaway, C. Melbourne, "Small and large-scale experimental studies of soil-arch interaction in masonry bridges", in *Proceedings of the 5th International Conference on Arch Bridges*, ARCH'07, Madeira, Portugal. 2007, pp. 381–388.
- [7] R. Royles, A.W. Hendry, "Model tests on masonry arches", *Proceedings of the Institution of Civil Engineers. Part 2. Research and Theory*, 1991, vol. 91, pp. 299–321, DOI: [10.1680/iicep.1991.14997](https://doi.org/10.1680/iicep.1991.14997).
- [8] R. Helmerich, E. Niederleithinger, C. Treila, J. Bień, T. Kamiński, G. Bernardini, "Multi-tool inspection and numerical analysis of an old masonry arch bridge", *Structure and Infrastructure Engineering*, 2015, vol. 8, no. 1, pp. 27–39, DOI: [10.1080/15732471003645666](https://doi.org/10.1080/15732471003645666).
- [9] G. Zani, P. Martinelli, A. Galli, M. Di Prisco, "Three-dimensional modelling of a multi-span masonry arch bridge: Influence of soil compressibility on the structural response under vertical static loads", *Engineering Structures*, 2020, vol. 221, DOI: [10.1016/j.engstruct.2020.110998](https://doi.org/10.1016/j.engstruct.2020.110998).
- [10] C. Costa, D. Ribeiro, P. Jorge, R. Silva, R. Calçada, A. Arêde, "Calibration of the numerical model of a short-span masonry railway bridge based on experimental modal parameters", *Procedia Engineering*, 2015, vol. 114, pp. 846–853, DOI: [10.1016/j.proeng.2015.08.038](https://doi.org/10.1016/j.proeng.2015.08.038).
- [11] A. Bayraktar, A.C. Altunışık, F. Birinci, B. Sevim, T. Türker, "Finite-element analysis and vibration testing of a two-span masonry arch bridge", *Journal of Performance of Constructed facilities*, 2010, vol. 24, no. 1, pp. 46–52, DOI: [10.1061/\(ASCE\)CF.1943-5509.0000060](https://doi.org/10.1061/(ASCE)CF.1943-5509.0000060).
- [12] C. Pepi, M. Gioffrè, G. Comanducci, N. Cavalagli, A. Bonaca, F. Ubertini, "Dynamic Characterization of a Severely Damaged Historic Masonry Bridge", *Procedia Engineering*, 2017, vol. 199, pp. 3398–3403, DOI: [10.1016/j.proeng.2017.09.579](https://doi.org/10.1016/j.proeng.2017.09.579).
- [13] A. Brencich, D. Sabia, "Experimental identification of a multi-span masonry bridge: the Tanaro Bridge", *Construction and Building Materials*, 2008, vol. 22, no. 10, pp. 2087–2099, DOI: [10.1016/j.conbuildmat.2007.07.031](https://doi.org/10.1016/j.conbuildmat.2007.07.031).
- [14] C. Costa, D. Ribeiro, P. Jorge, et al., "Calibration of the numerical model of a stone masonry railway bridge based on experimentally identified modal parameters", *Engineering Structures*, 2016, vol. 123, pp. 354–371, DOI: [10.1016/j.engstruct.2016.05.044](https://doi.org/10.1016/j.engstruct.2016.05.044).
- [15] B. Conde, L.F. Ramos, D.V. Oliveira, et al., "Structural assessment of masonry arch bridges by combination of non-destructive testing techniques and three-dimensional numerical modeling: Application to Vilanova bridge", *Engineering Structures*, 2017, vol. 148, pp. 621–638, DOI: [10.1016/j.engstruct.2017.07.011](https://doi.org/10.1016/j.engstruct.2017.07.011).
- [16] C. Pepi, N. Cavalagli, V. Gusella, M. Gioffrè, "An integrated approach for the numerical modeling of severely damaged historic structures: Application to a masonry bridge", *Advances in Engineering Software*, 2021, vol. 151, DOI: [10.1016/j.advengsoft.2020.102935](https://doi.org/10.1016/j.advengsoft.2020.102935).
- [17] M. Yazdani, P. Azimi, "Assessment of railway plain concrete arch bridges subjected to high-speed trains", *Structures*, 2020, vol. 27, pp. 174–193, DOI: [10.1016/j.istruc.2020.05.042](https://doi.org/10.1016/j.istruc.2020.05.042).
- [18] A. Bayraktar, T. Türker, A.C. Altunışık, "Experimental frequencies and damping ratios for historical masonry arch bridges", *Construction and Building Materials*, 2015, vol. 75, pp. 234–241, DOI: [10.1016/j.conbuildmat.2014.10.044](https://doi.org/10.1016/j.conbuildmat.2014.10.044).

- [19] J. Bień, J. Zwolski, T. Kamiński, J. Rabiega, P. Rawa, M. Kużawa, "Dynamic tests of two old masonry arch bridges over Odra River in Wrocław", in *4th International Conference on Experimental Analysis for Civil Engineering Structures*, EVACES 2011, Varenna, Włochy. 2011, pp. 79–86.
- [20] S. Ataei, M.J. Alikamar, V. Kazemiastian, "Evaluation of Axle Load Increasing on a Monumental Masonry Arch Bridge Based on Field Load Testing", *Construction and Building Materials*, 2016, vol. 116, pp. 413–421, DOI: [10.1016/j.conbuildmat.2016.04.126](https://doi.org/10.1016/j.conbuildmat.2016.04.126).
- [21] S. Ataei, A. Miri, "Investigating dynamic amplification factor of railway masonry arch bridges through dynamic load tests", *Construction and Building Materials*, 2018, vol. 183, pp. 693–705, DOI: [10.1016/j.conbuildmat.2018.06.151](https://doi.org/10.1016/j.conbuildmat.2018.06.151).
- [22] C. Machelski, "Stiffness of railway soil-steel structures", *Studia Geotechnika et Mechanica*, 2015, vol. 37, no. 4, pp. 29–36, DOI: [10.1515/gem-2015-0042](https://doi.org/10.1515/gem-2015-0042).
- [23] O. Burdet, S. Corthay, "Static and dynamic load testing of Swiss bridges", in *Proceedings of the International Bridge Conference*, vol. 2. Warszawa, 1994, pp. 13–22.
- [24] C. Machelski, "The use of the collocation algorithm for estimating the deformation of soil-shell objects made of corrugated sheets", *Studia Geotechnika et Mechanica*, 2020, vol. 42, no. 4, pp. 319–329, DOI: [10.2478/gem-2019-0048](https://doi.org/10.2478/gem-2019-0048).
- [25] J. Orkisz, "Finite Difference Method (part III)", in: *Handbook of Computational Solid Mechanics*, M. Kleiber, Ed. Springer-Verlag, 1998, pp. 336–431.
- [26] T. Kamiński, "Mezomodelling of masonry arches", *6th International Conference AMCM'2008 – Analytical Models and New Concepts in Concrete and Masonry Structures*, 9–11 June 2008, Łódź, 9–11 June. 2008, pp. 359–360.
- [27] P.B. Lourenço, "The elastoplastic implementation of homogenisation techniques". Delft University of Technology Report, TNO-95-NM-R0251, 1995.

Analiza efektów obciążen użytkowych w kolejowych mostach sklepionych

Słowa kluczowe: analiza numeryczna, badania terenowe, linie wpływów, Metoda Elementów Dyskretnych, Metoda Elementów Skończonych, murowany most sklepiony

Streszczenie:

Artykuł skupia się na zagadnieniu przemieszczeń sklepień mostów murowanych wywołanych ich typowymi obciążeniami użytkowymi. Szczególna uwaga zwrócona jest na pomiar przemieszczeń pionowych i radialnych w charakterystycznych punktach sklepienia. W przedstawionych przykładach rozpatrzone zachowanie jedno- i wieloprzęsłowych mostów łukowych opartych na sklepieniach murowanych i betonowych pod obciążeniem przejeżdżającymi pojazdami kolejowymi różnego rodzaju.

Na podstawie otrzymanych wyników pomiarów terenowych prowadzonych na powyższych obiektach stworzono doświadczalne funkcje wpływu przemieszczeń. W kolejnym kroku uzyskane wyniki wykorzystywane są do wyznaczenia momentów zginających w sklepieniu.

W artykule przedstawiono odmienne procedury postępowania bazujące na pomiarach przemieszczeń w różnych kierunkach i w różnie rozmieszczonych punktach. Szczególną zaletą przedstawionego całościowego podejścia jest możliwość wykonania pożądanych pomiarów podczas standardowej eksploatacji mostu bez jakiegokolwiek zakłócania ruchu taboru, co w wielu sytuacjach czyni przeprowadzenie tego typu badań w ogóle możliwymi. Przyjęte schematy postępowania są szczególnie skuteczne w przypadku obiektów kolejowych charakteryzujących się regularnością i łatwością w identyfikacji ich schematów obciążen reprezentowanych zwłaszcza przez lokomotywy. Niemniej jednak przedstawione podejście może być wykorzystane również w analizie mostów drogowych. Podane

procedury mogą opierać się też na innych efektach statycznych (przemieszczeniach i odkształceń w dowolnych kierunkach) mierzonych w dowolnych punktach konstrukcji. Zaproponowaną metodykę można wykorzystywać, co również zobrazowano w artykule, jako efektywne narzędzie do wszechstronnej kalibracji modeli numerycznych mostów sklepionych obejmującej np. weryfikację ich parametrów materiałowych, niewidocznej geometrii czy, w przypadku modeli dwuwymiarowych, ich szerokości efektywnej.

Received: 30.11.2021, Revised: 01.12.2021